Square-wave Voltammetry of Two-step Surface Electrode Mechanisms Coupled with Chemical Reactions – a Theoretical Overview

Milkica Janeva,[a] Pavlinka Kokoskarova,[a] Viktorija Maksimova,[a] and Rubin Gulaboski*[a]

Abstract: Square-wave voltammetry (SWV) of so-called "surface redox reactions" is seen as a simple and efficient tool to quantify large number of drugs, physiologically active substances and other important chemicals. It also provides elegant methods to get access to relevant kinetic and thermodynamic parameters related to many lipophilic compounds. Moreover, with this technique we can study activity of various enzymes by exploring the "protein-film voltammetry" set up. In this work, we focus on theoretical SWV features of four complex surface electrode mechanisms, in which the electron exchange between the working electrode and the studied redox substrate takes place in two successive steps. While we present large number of calculated square-wave voltammograms, we give hints to recognize particular two-step surface mechanism, but also to distinguish it from other similar mechanisms. We present plenty of relevant aspects of surface two-step surface EE, two-step surface ECE and surface catalytic EEC' mechanisms. Moreover, we present for the first time a series of theoretical results related to two-step surface EECrev mechanism (i.e. two-step surface reaction coupled to follow-up reversible chemical step). The simulated voltammetric patterns presented in this work can bring relevant aspects to resolve some experimental situations met in voltammetry of many redox enzymes and other important substances whose electrochemical transformation occurs in two-steps.

Keywords: electron transfer reactions coupled with chemical reactions · protein-film voltammetry · two-step mechanisms · surface EE reactions · kinetics of chemical reactions

1 Introduction

Many lipophilic enzymes [1–9], drugs and other physiologically relevant compounds [10–19] feature so-called "active centers" in their structures that can undergo redox transformation in a successive stepwise fashion. Of these, significant interest attract biological systems containing quinine/hydroquinone moiety [20], or some polyvalent cations as that of Mo, V, Cr or Mn [21–24] as redox active center in their structures. The redox chemistry of many of these systems can be successfully addressed by exploring voltammetric techniques, provided their redox active center(s) can exchange electrons with the working electrode under controlled bias. In the last 25 years, the technique named "protein-film voltammetry" emerges as one of the most suitable tools to get insight into the redox chemistry of many lipophilic enzymes and other "surface-active" compounds [1–9,12–14]. This technique considers voltammetric experiments in which a small amount of given lipophilic redox enzyme or surface-active compound adsorbs strongly at the working electrode. The molecules of redox active system studied form a well-defined monolayer at the working electrode surface. In the next step, the working electrode, modified with monolayer of molecules of considered substance, gets introduced in an electrolyte solution that might contain a defined substrate, too. Afterwards, by applying a controlled potential from external source, we can perform usual electrochemical experiments in a common three-electrode voltammetric set-up [1–9,12–14,18,19]. From the voltammetric outputs recorded in such scenario, we can get many relevant information about the chemistry of many important compounds [2,8–14]. In the last two decades, this methodology is successfully explored to quantify important compounds and to determine kinetic and thermodynamic parameters relevant to relevant lipophilic biological systems that undergo successive multi-step redox transformation [5–16]. Moreover, our group [8–16,25–38] and others [17–19,39–59] presented several theoretical models under voltammetric conditions that provide a basis for designing simple methods to recognize a particular electrode mechanism. In addition, plenty of simple methods are provided in our theoretical works [8–16,25–38] allowing elegant access to kinetic and thermodynamic parameters relevant to many lipophilic redox active systems. This work focuses on the use of square-wave voltammetry to characterize theoretically several two-step surface electrode mechanisms coupled with chemical reactions. The major emphasis in this theoretical overview

[a] M. Janeva, P. Kokoskarova, V. Maksimova, R. Gulaboski
Faculty of Medical Sciences, Goce Delcev University, Stip, Macedonia
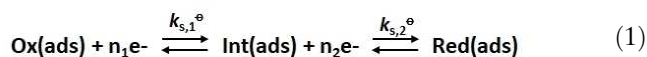E-mail: rubin.gulaboski@ugd.edu.mk

is on providing diagnostic criteria for recognizing particular two-step surface electrode reaction, and to distinguish it from other similar electrode reactions. We also provide hints on how to recognize a particular two-step surface electrode mechanism, in a complex scenario when both electron transfer steps occur at a very same potential. Moreover, at the two-step surface redox reactions coupled to chemical steps, we give hints to several methodologies that allow access to kinetic and thermodynamic parameters of considered coupled chemical reactions from time-independent voltammetric experiments. It is worth to mention that there is only limited number of theoretical works focused on square-wave voltammetry of two-step redox mechanisms published so far [8,9,12,14,25–27,38,40,42,45,47,52,53].

2 Mathematical Models

In our four theoretical models elaborated in this work, we consider two-step electrode mechanisms of redox active adsorbates, whose molecules are uniformly adsorbed to the working electrode surface, i.e.:
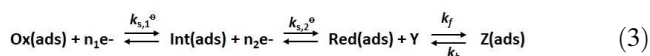
(1) "Simple" two-step surface redox reaction or "*surface EE mechanism*"

$$\text{Ox(ads)} + n_1e\text{-} \underset{}{\overset{k_{s,1}^{\ominus}}{\rightleftharpoons}} \text{Int(ads)} + n_2e\text{-} \underset{}{\overset{k_{s,2}^{\ominus}}{\rightleftharpoons}} \text{Red(ads)} \quad (1)$$

(2) Two-step surface redox reaction cross-linked with an irreversible (irr) chemical step, i.e. surface ECirrE or simply "*surface ECE mechanism*"

$$\text{Ox(ads)} + n_1e\text{-} \overset{k_{s,1}^{\ominus}}{\rightleftharpoons} \text{Int1(ads)} + Y \overset{k_{chem}}{\rightarrow} \text{Int2(ads)} + n_2e\text{-} \overset{k_{s,2}^{\ominus}}{\rightleftharpoons} \text{Red(ads)} \quad (2)$$

(3) Two-step surface redox reaction coupled to reversible follow-up chemical step to last product of electrode reaction, or "*surface EECrev mechanism*"

$$\text{Ox(ads)} + n_1e\text{-} \overset{k_{s,1}^{\ominus}}{\rightleftharpoons} \text{Int(ads)} + n_2e\text{-} \overset{k_{s,2}^{\ominus}}{\rightleftharpoons} \text{Red(ads)} + Y \underset{k_b}{\overset{k_f}{\rightleftharpoons}} \text{Z(ads)} \quad (3)$$

(4) Two step surface redox reaction with irreversible catalytic chemical step coupled to last product of electrode reaction, or "*surface catalytic EEC' mechanism*"

$$\text{Ox(ads)} + n_1e\text{-} \rightleftharpoons \text{Int(ads)} + n_2e\text{-} \overset{k_{s,2}^{\ominus}}{\rightleftharpoons} \text{Red(ads)} + Y \overset{k_c'}{\rightarrow} \text{Int(ads)} \quad (4)$$

The term "E" stands for the electron transfer step between the working electrode and a given substance adsorbed on it, while the term "C" means chemical reaction. At the beginning of the experiment, only Ox species are present in the electrochemical cell and they get uniformly adsorbed to the working electrode surface. With *Int(ads)* (or *Int1(ads)* in the surface ECE mechanism*)* we assign intermediate species created upon reduction of Ox(ads) in first electrode step. *Red(ads)* species are the ultimate redox active species, generated

electrochemically in the course of second electrode transfer step. By "*Y*" we define an electrochemically non-active compound (in the potential region used). Y can react irreversibly with *Int1(ads)* creating *Int2(ads)* redox species in the surface ECE mechanism (2), or it can react in a chemically reversible fashion with Red(ads) species, converting them to final electrochemically inactive product *Z(ads)* in electrode mechanism (3). In last electrode mechanism (surface catalytic EEC'), "Y" reacts irreversibly with Red(ads), in a way of regenerating *Int(ads)* intermediate redox active species. In all elaborated mechanisms, we assume that "Y" substrate is present in large excess in the electrochemical cell, and it shows no electrochemical activity at the working electrode in the frame of applied potentials. Therefore, the concentration of "Y" remains constant at the electrode surface during the voltammetric experiments. Consequently, we assume that the chemical steps in all considered two-step mechanisms (2–4) are of pseudo-first order. Elaborated mechanisms (1–4) are solved under following conditions:

$t = 0$; $\Gamma(\text{Ox}) = \Gamma^*(\text{Ox})$; $\Gamma(\text{Int}) = \Gamma(\text{Int1}) = \Gamma(\text{Int2}) = \Gamma(\text{Red}) = 0$ (holds for all mechanisms $1 - 4$)

$t > 0$; $\Gamma(\text{Ox}) + \Gamma(\text{Int}) + \Gamma(\text{Red}) = \Gamma^*(\text{Ox})$
(holds for mechanisms 1 and 4)

$t > 0$; $\Gamma(\text{Ox}) + \Gamma(\text{Int1}) + \Gamma(\text{Int2}) + \Gamma(\text{Red}) = \Gamma^*(\text{Ox})$
(holds for mechanism 2)

$t > 0$; $\Gamma(\text{Ox}) + \Gamma(\text{Int}) + \Gamma(\text{Red}) + \Gamma(\text{Z}) = \Gamma^*(\text{Ox})$
(holds for mechanism 3)

For $t > 0$, the following conditions apply to considered mechanisms (1–4):

$d\Gamma(\text{Ox})/dt = -I_1/(n_1FS)$
(holds for all mechanisms $1 - 4$)

$d\Gamma(\text{Int})/dt = I_1/(n_1FS) - I_2/(n_2FS)$
(holds for mechanisms 1 and 3)

$d\Gamma(\text{Int1})/dt = I_1/(n_1FS) - k_c\Gamma(\text{Int1})$
(holds for mechanism 2)

$d\Gamma(\text{Int2})/dt = I_2/(n_2FS) + k_c\Gamma(\text{Int1})$
(holds for mechanism 2)

$d\Gamma(\text{Int})/dt = I_1/(n_1FS) - I_2/(n_2FS) + k_c\Gamma(\text{Red})$
(holds for mechanism 4)

$d\Gamma(\text{Red})/dt = I_2/(n_2FS)$
(holds for mechanism 1)

$d\Gamma(\text{Red})/dt = I_2/(n_2FS) - k_f\Gamma(\text{Red}) + k_b\Gamma(\text{Z})$
(holds for mechanism 3)

$d\Gamma(\text{Red})/dt = I_2/(n_2FS) - k_c\Gamma(\text{Red})$
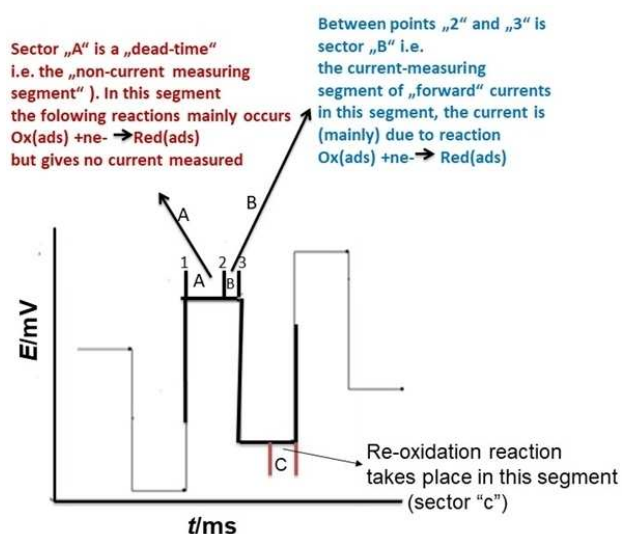(holds for mechanism 4)

In all models, we consider a Buttler-Volmer formalism holding for the interdependence between the potential applied, electric current, the surface concentrations (Γ) of all species involved, and the electrode reaction parameters that affect the features of theoretical voltammograms. The analytical solution of electrode mechanism (1) the surface EE mechanism under conditions of SWV is given in [12]. In [25] and [26] we find the analytical solutions of mechanisms (2) (the surface ECE mechanism) and (4) (the surface catalytic EEC' mechanism), respectively. Since the electrode mechanism (3) is presented for the first time in this work, in the supplementary material in this work we give a detailed MATHCAD file containing all recurrent formulas for calculating theoretical voltammograms of surface EECrev mechanism (3). In all models considered, we define the reduction currents to have positive sign, while negative sign is ascribed to oxidation currents. All potentials are defined vs. the standard redox potential of the first electrode process that happens at more positive potentials (assigned as "Peak I"). In all simulations, the starting potential is set to positive value, and it runs toward final negative potentials. The potential form of a given square-wave pulse, together with short explanations of processes going on in every important segment at the pulse, is given in Scheme 1.

3 Parameters Affecting the Features of Calculated Voltammograms

The total dimensionless current of theoretical SW voltammograms in all models is defined as a sum of currents related to the first and the second electrode step, i.e. $\Psi = \Psi_I + \Psi_{II}$. The particular dimensionless currents relevant to both electrode steps are defined as $\Psi_I = I_1/[(n_1 FSf\Gamma(\mathrm{Ox})^*)]$ and $\Psi_{II} = I_2/[(n_2 FSf\Gamma(\mathrm{Ox}))]$. With I we define the electric current, while n_1 and n_2 are the numbers of electrons exchanged in the first and the second electrode step, respectively. In all calculations, we set $n_1 = n_2 = n = 1$. S is the active area of working electrode, while f is the SW frequency defined as $f = 1/(2t_p)$, where time parameter t_p is defined as duration of a single potential pulse in SWV. "Γ" is a symbol of the surface concentration. With $\Gamma(\mathrm{Ox})^*$ we define the total surface concentration, which is, in fact, the initial surface concentration of adsorbed Ox species. Φ is a symbol of dimensionless potential defined as $\Phi_1 = nF(E - E_1^{\circ'}/RT)$ and $\Phi_2 = nF(E - E_2^{\circ'}/RT)$, where $E_1^{\circ'}$ and $E_2^{\circ'}$ are the standard (or more precisely, the formal) redox potentials of first and second electrode step, respectively. α is a symbol for the electron transfer coefficient. We set in all calculations α to value of 0.5 for both electrode transfer steps. By T we define the thermodynamic temperature (it was set to 298 K in all simulations), while R is the universal gas constant, and F is the Faraday constant. In addition, calculated SW voltammograms in all considered mechanisms are affected by several dimensionless parameters. The dimensionless electrode kinetic parameters $K\mathrm{I} = k_{s,1}^{\circ}/f$ and $K\mathrm{II} = k_{s,2}^{\circ}/f$ reflect the influence of standard rate constants of both electrode steps ($k_{s,1}^{\circ}$ and $k_{s,2}^{\circ}$) to the time duration of potential pulses in SWV. For the surface ECE mechanism, calculated voltammograms are affected by a dimensionless chemical parameter K_{chem} defined as $K_{\mathrm{chem}} = k_{\mathrm{chem}}/f$. In the last equation, k_{chem} is the rate constant of irreversible chemical reaction in mechanism (2). For the surface EECrev mechanism (3), the SW voltammograms are affected by a dimensionless chemical parameter K_{chem}, too, but defined slightly different than in mechanism (2). It is defined as $K_{\mathrm{chem}} = \varepsilon/f$, where $\varepsilon = (k_{\mathrm{f}} + k_{\mathrm{b}})$ is the sum of the first order rate constant k_{f} and k_{b} of the forward and backward chemical reaction, respectively. This dimensionless parameter in surface EECrev mechanism reflects the rate of the chemical step relative to the timeframe of current measurement in SWV. Moreover, the features of theoretical SW voltammograms of surface EECrev mechanism (3) depend on equilibrium constant K_{eq} that is defined as $K_{\mathrm{eq}} = k_{\mathrm{f}}/k_{\mathrm{b}}$. For the surface catalytic EEC' mechanism (4), the dimensionless chemical kinetic parameter affecting the features of calculated SW voltammograms is defined as $K_{\mathrm{chem}} = k_{\mathrm{c}}'/f$, where k_{c}' is the first order rate constant of the regenerative (catalytic) chemical reaction. At this stage, it is worth to emphasize that all chemical parameters k_{chem}, ε and k_{c}' in mechanisms (2–4) are of pseudo-first order since they all depend on the concentration of substrate "Y, $c(\mathrm{Y})$ in following manner: $k_{\mathrm{c}} = k_{\mathrm{c}}^{\circ}\,c(\mathrm{Y})$ for mechanism (1); $\varepsilon = [k_{\mathrm{f}}^{\circ}c(\mathrm{Y}) + k_{\mathrm{b}}]$ for mechanism (3); and $k_{\mathrm{c}}' = k_{\mathrm{c}}^{\circ}\,c(\mathrm{Y})$ for mechanism (4). In last equations, k_{c}°, k_{f}° and $k_{\mathrm{c}}^{\circ'}$ are real chemical rate constants in the corresponding mechanisms (2), (3) and (4), respectively.

In all simulations, the parameters of applied potential were set to: SW frequency $f = 10$ Hz, SW amplitude $E_{\mathrm{sw}} = 50$ mV, and potential step $dE = 4$ mV. More details of the algorithms used can be found in the Supplementary of

Sector „A" is a „dead-time" i.e. the „non-current measuring segment"). In this segment the folowing reactions mainly occurs Ox(ads) +ne- → Red(ads) but gives no current measured

Between points „2" and „3" is sector „B" i.e. the current-measuring segment of „forward" currents in this segment, the current is (mainly) due to reaction Ox(ads) +ne- → Red(ads)

Re-oxidation reaction takes place in this segment (sector "c")

Scheme 1. Features of one square-wave voltammetric pulse, with explanation of some of the processes happening in defined segments of the SWV pulse.

this work and in references [25,27]. We used MATHCAD 14 software for calculating the SW voltammograms in all considered mechanisms (1–4). The net current in all simulated voltammetric patterns is represented by black colour, while the forward (reduction) currents are assigned with blue colour. Red colour is associated with the backward (reoxidation) current branches at all simulated voltammograms.

4 Results and Discussion

Before we start elaborating some specific features of coupled surface two-step mechanisms in SWV, it is worth to mention several aspects important to all electrode mechanisms coupled with chemical reactions. The term "coupling" refers to a chemical process that commonly makes thermodynamically more favorable a given electron transfer step between the working electrode and the redox adsorbate of interest. Protonation, for example, is one chemical process that is often coupled to electron transfer steps. While the fast coupled chemical reaction might influence the thermodynamics of the electrode reaction (by displacing the redox equilibrium), the slow chemical reaction may affect the rate of the overall reaction. Indeed, when we talk about fast or slow chemical reaction rates in voltammetry, it is important to understand that the terms "fast" or "slow" are always relative, since they depend on the time scale at potential pulse where the current is measured in SWV. In this work, we focus mainly on the effect of chemical kinetics rate to the SW voltammetric patterns featuring various kinetics at both electrode steps. As defined in previous section, the dimensionless chemical rate parameters at all considered mechanisms are affected both by the SW frequency and by the concentration of substrate "Y". Since the SW frequency affects not the chemical rates only, but also the rates of both electrode steps (via KI and KII), we point out here that all calculations are performed at a constant SW frequency f. This means, we consider in our simulations mainly the effect of concentration of "electrochemically inactive" substrate "Y"-c(Y) to the features of calculated SW voltammetric patterns.

4.1 A. Surface EE Mechanism

We first consider the situation where the current-potential response reveals a direct electron transfer happening in two consecutive steps between the electrode and the redox centers of strongly adsorbed molecules, in absence of chemical reaction. In all mechanisms considered in this work, we will elaborate two cases: (I) scenario of well-separated SW peaks of first and second electrode step (separated at least 300 mV at potential scale); and (II) scenario where both electrode steps happen at a very same potential, which will be reflected in a single voltammetric peak.

4.1.1 I. Surface EE Mechanism with Two Separate Electrode Steps for at Least 300 mV

Shown in Figure 1a–d is a series of theoretical square-wave voltammograms of a simple two-step surface reaction (mechanism 1), simulated for several values of dimensionless electrode kinetic parameters KI and KII. When the electrode potential is suitable, electrons get exchanged between the molecules of studied redox adsorbates and the working electrode. The magnitude of the current measurement should be proportional to the turnover rate of electroactive material available at the working electrode surface. Initially, an increase of the electron transfer rate is followed by considerable gain of the magnitude in all current components at both SW peaks (Figure 1a–b). As the maximum peak currents are reached for KI and KII ≈ 0.6 (Figure 1b), all current components start to decrease by further increasing of K values (Figure 1c–d). For KI and KII > 0.5 we observe shifting of cathodic (forward) peaks at both SW peaks to more positive potential values, while anodic (backward) peaks shift in opposite direction. Final output of these events is splitting of both net SWV peaks (Figure 1d). Well-recognizable features of all surfaces redox reactions are "quasireversible maximum" and "splitting of net SWV peak" [10]. The quasireversible maximum is phenomenon of net-SW peak current parabolic dependence as a function of logarithm of dimensionless kinetic parameter related to the electrode reaction K. It is a consequence of synchronizing the rate of the electron transfer step with the measuring timeframe at potential pulses in SWV. This phenomenon leads to optimal and multiple reuse the electroactive material at quasireversible reactions (i. e. electrode reactions featuring moderate rate of electron transfer), which feature maximal measured net currents [10]. The "net SWV peak-splitting" phenomenon is met by the surface electrode reactions with very fast kinetics of electron transfer step [8–16,29,32–37]. Very fast surface redox reactions require short time for the redox transformation of Ox(ads) to Red(ads). This, in turn, produces only minute amount of electroactive redox adsorbates remaining in the short time segment of current measurement at given potential pulses in SWV (Scheme 1). Consequently, the current detected at the end of SW potential pulses of fast surface electrode reactions will be very small as shown in Figure 1d. By both SW peaks of a surface EE mechanism (when separated for 300 mV or more), we can explore the phenomena of "quasireversible maximum" and "splitting of net SW peak" to get access to rate constants of both electron transfer steps as elaborated in [10,13–16].

4.1.2 II. Surface EE Mechanism with Two Electrode Steps Taking Place at Same Potential

Shown in Figure 2a–d is a situation of a surface EE mechanism, when both electrode steps occur at a very same potential. This scenario happens when the energy of
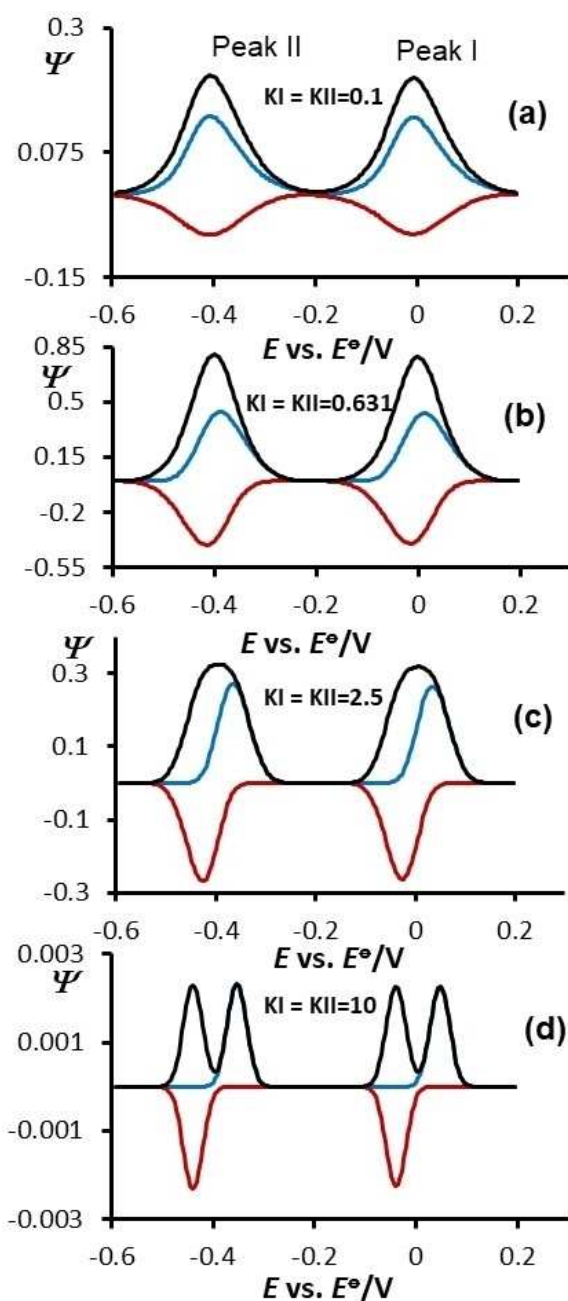
Fig. 1. **Surface EE mechanism**: Square-wave voltammetric patterns simulated at potential separation of −400 mV between the two electrode steps: Effect of the values of both dimensionless kinetic parameters KI and KII to the features of simulated SW voltammograms. The values of KI and KII are given in the charts. Other simulation parameters were: SW frequency f = 10 Hz, SW amplitude E_{sw} = 50 mV, potential step dE = 4 mV, temperature T = 298 K. In all simulations, the electron transfer coefficients of first and second electrode reaction was set to α = 0.5, while the number of electron exchanged between working electrode and the redox adsorbates was $n_1 = n_2 = 1$.

Fig. 2. *Surface EE mechanism: Square-wave voltammetric patterns simulated for both electrode steps taking place at same potential:* Effect of both dimensionless kinetic parameters KI and KII to the features of simulated SW voltammograms. The values of KI and KII are given in the charts. Other simulation parameters were same as in Figure 1.

occurring of second electrode step is less or equal than that of the first electrode step. The final output of such a sequence of events is portrayed in a single voltammetric SW peak having almost the same features as voltammetric

outputs of one-step surface electrode reactions. Indeed, a major challenge in such scenario is to find criteria and to recognize whether the SW voltammogram belongs to a "one-step" surface electrode reaction, or it is due to a two-step consecutive surface EE mechanism. This is, indeed, not an easy task. In the next elaborated two-step surface mechanisms of this work we gonna give hints on how to distinguish a one-step surface electrode mecha-

nism from the two-step surface EE mechanism, when both electrode steps of the surface EE mechanisms occur at same potential.

4.2 B. Surface ECE Mechanism

4.2.1 III. Surface ECE Mechanism with Two Separate Electrode Steps for at Least 300 *mV*

Figure 3 shows effect of the rate of chemical reaction at a surface ECE mechanism when both electrode steps fall in the quasireversible region of electron transfer ($KI = KII = 0.1$).

Under such circumstances, the magnitude of all current components of second electrode step is determined by the rate of chemical reaction. If the rate of chemical step, which consumes the product of first electrode step and converts it to a reactant for second electrode step is small, then we see minute currents measured for the second electrode reaction, regardless of the value of KII (Figure 3a). As the rate of irreversible chemical reaction increases, then we see enlargement of all current components of second voltammetric peak (Peak II), and concomitant decrease of all currents measured by the first voltammetric peak (Peak I) (see Figure 3b–d). In such sequence of events, the first peak has attributes of a surface EC_{irr} ("irr" is abbreviation for irreversible) reaction, while the features of the second peak can be ascribed as those to a surface $C_{irr}E$ process. Indeed, if both SW peaks of a surface ECE mechanism are nicely separated, and the electrode kinetics of both steps fall in the quasireversible region of electron transfer, then one can explore the methods elaborated in [10,14,25,27] for getting access to all parameters relevant to this mechanism.

Situation gets much more complicated when both separated SWV peaks of a surface ECE mechanism feature fast kinetics at both electrode steps (situation of split net SWV peaks, Figure 4a–f). In such scenario, we see very interesting phenomenon in the region of chemical rates $0.01 < K_{chem} < 0.2$ (see Figure 4b–d). In the mentioned region of K_{chem} values, an increase of the rate of irreversible chemical reaction leads to simultaneous increase not only by the current of second electrode process (Peak II), but also at all SWV current components of first electrode process. What is even more intriguing, the backward (re-oxidation) SW current components of first electrode process (the one that should be "consumed" by the chemical reaction) rises more intensively than the forward one by increasing K_{chem} (see Figure 4b–c). For instance, the ratio of the absolute values of backward (reoxidation) *vs.* forward (reduction) peak currents of first electrode step increases permanently in the region $0.01 < K_{chem} < 0.2$ and reaches a maximal value of 1.40 for K_{chem} of about 0.075 (see Figure 4c). In the same time, reduction (forward) peak of the first electrode process shifts to more negative potentials by increasing the value of K_{chem}. The final output of these events is
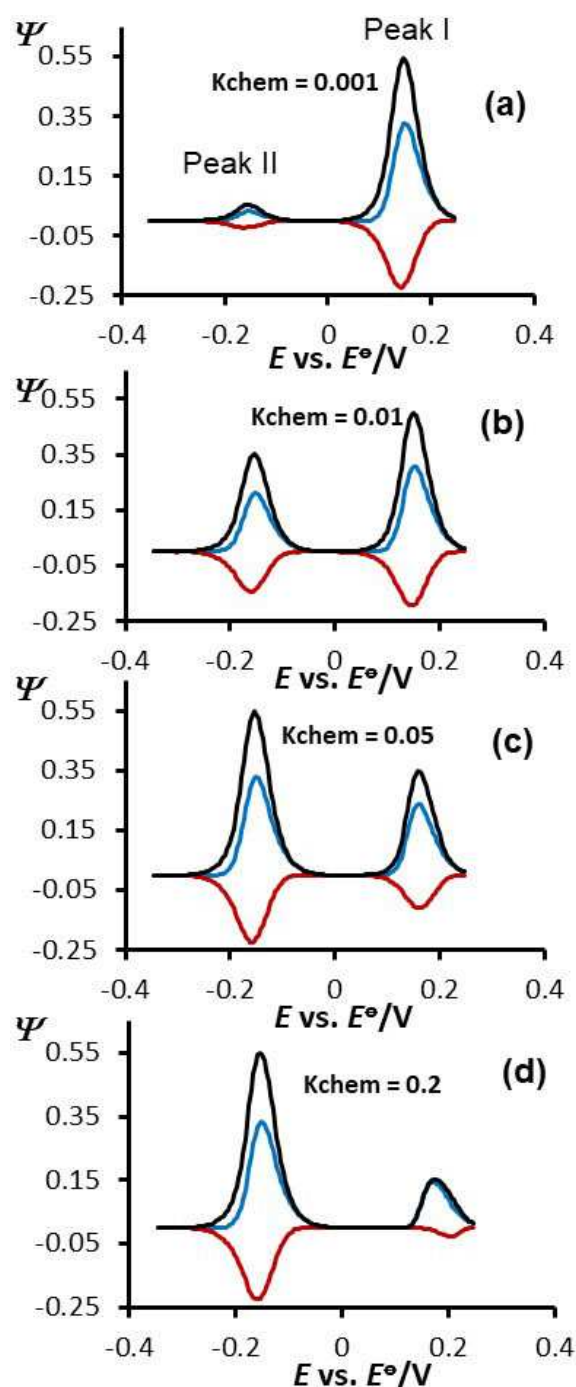

Fig. 3. **Surface ECE mechanism**: Square-wave voltammetric patterns simulated at potential separation of -400 mV between the two electrode steps: Effect of the chemical kinetic parameter K_{chem} to the features of simulated SW voltammograms. The values of K_{chem} are given in the charts. In all simulations, the values of KI and KII were set to 0.1. Other simulation parameters were same as in Figure 1.

portrayed in vanishing the net current splitting phenomenon at Peak I (see Figure 4c–d), that leads to existence of a single net SWV peak. Eventually, for values of $K_{chem} > 0.2$, we observe decrease of all current components
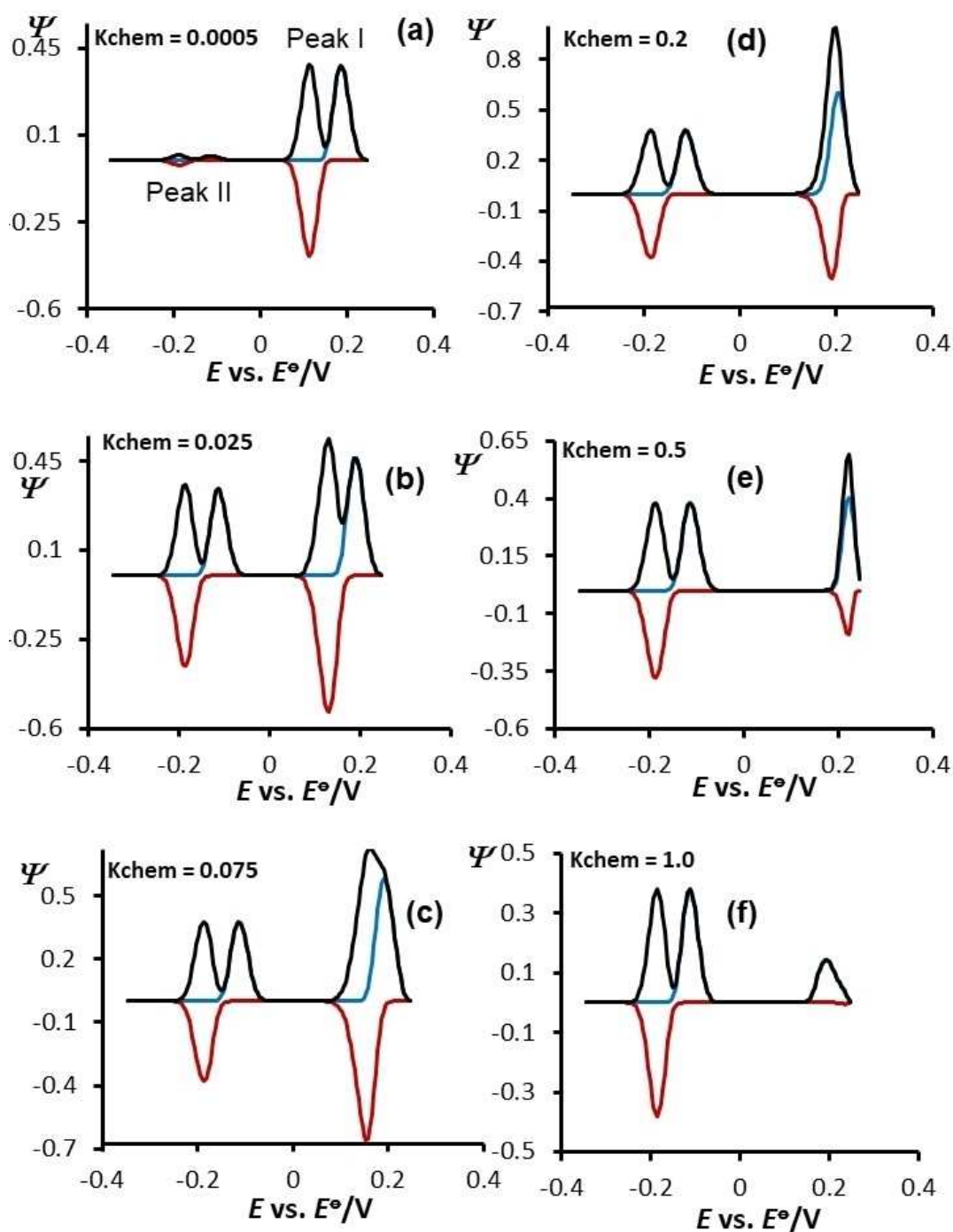
Fig. 4. Surface ECE mechanism: Square-wave voltammetric patterns simulated at potential separation of $-400\,mV$ between the two electrode steps: Effect of dimensionless chemical kinetic parameter K_{chem} to the features of simulated SW voltammograms. The values of K_{chem} are given in the charts. In all simulations, the values of KI and KII were set to 2. Other simulation parameters were same as in Figure 1.

of first SWV peak, as expected for an ECirr reaction (Figure 4d–f). As explained in [27,29,35], the phenomenon of increase of all SWV current components at surface EC reactions by increasing the rate of follow-up chemical reaction is due to specific chronoamperometric features of these mechanisms in SWV. The so-called "dead-time" in each potential SW pulse [35] is a segment where the current is not measured (see Scheme 1).

As shown in Scheme 1, in "dead-time" segment of each potential SW pulse both the redox electrode transformation as well as the chemical reaction happen, too. Such a series of events that occurs in the "dead time" of given potential SW pulses produces significant disturb-

ance in the equilibrium of redox adsorbates [35]. This happens when kinetics of electrode reaction is comparable to the rate of chemical transformation. Such an event creates more "electroactive" material available for electrode transformation in the current measuring time-segment of given SW pulses. A turnout of these phenomena will be depicted in higher SWV currents detected at moderate rates of follow-up chemical reaction as explained in [27,29,35].

4.2.2 IV. Surface ECE Mechanism with Both Electrode Steps Taking Place at Same Potential

Shown in Figures 5 and 6 is a series of calculated SW voltammograms of a surface ECE mechanism. These voltammetric patterns portray the effect of the rate of irreversible chemical reaction, simulated for two set of different electrode kinetics parameters. As the rates of both electrode steps fall in quasireversible region (Figure 5), then we observe SW voltammograms with features typical as those of a surface EC_{irr} reaction [35]. In such scenario, the net SW peak shifts towards more positive potentials by increasing K_{chem} for 59 mV/[log(K_{chem})], in the region of $0.005 < K_{chem} < 0.1$. On the other side, as K_{chem} increases, all SWV current components decrease in their peak heights, with more pronounced decrease of the backward (oxidation) peak currents (Figure 5b–d). The surface ECE mechanism can be formally considered to consist of one surface EC_{irr} process coupled with additional surface $C_{irr}E$ step. Since both electrode processes in Figure 5 occur at a very same potential, and because the entire electroactive material remains adsorbed at the working electrode surface, one expects that the rate of chemical reaction should not have dramatic impact to the features of net SW voltammograms in such scenario. Again, explanation for phenomena observed in Figure 5 should be find in specific chrono-amperometric features of this mechanism in SWV [35]. When both electrode processes of a surface ECE mechanism occur at same potential, then both "redox" equilibria at working electrode surface can be significantly disturbed during the "dead time" of given potential SW pulses. In the dead-time segment of SW potential pulses, moderate rates of chemical reaction might lead to production of significant amount of final redox product Red(ads). This event will lead to a small amount of Ox(ads) remaining in the current measuring time-frame in the end of SW potential pulses (see Scheme 1). This sequence of events in the surface ECE mechanism will lead to significant current diminishment due to small amount of initial electroactive material prone to undergone transformation during the small time-window of current measurement in SW pulses. Probably, this is one of the reasons for the features of calculated SW voltammograms reported in Figure 5.

However, when both KI and KII are very big (scenario of split net SWV peaks), then the features of calculated SW voltammograms resemble in many aspects to both,
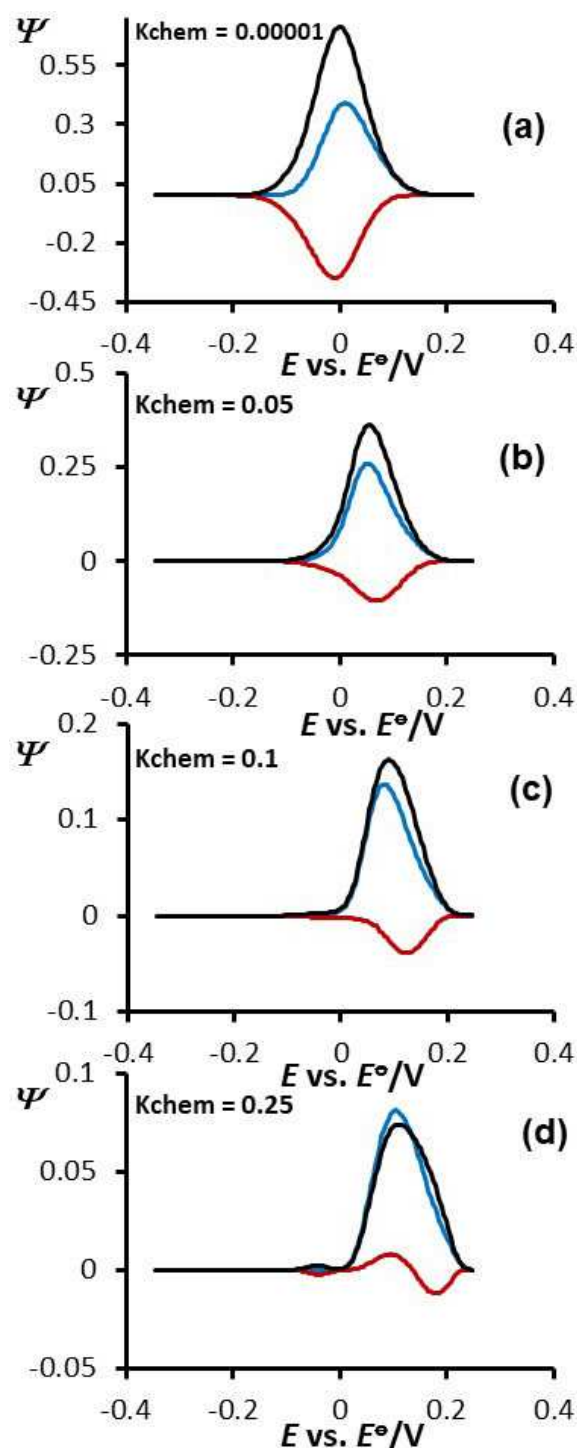

Fig. 5. *Surface ECE mechanism*: Square-wave voltammetric patterns simulated for both electrode steps taking place at same potential: Effect of chemical kinetic parameter K_{chem} to the features of simulated SW voltammograms. The values of K_{chem} are given in the charts. In all simulations, the values of KI and KII were set to 0.5. Other simulation parameters were same as in Figure 1.

the simple surface EC_{irr} mechanism [35] and the simple surface $C_{irr}E$ mechanism [31] (see Figure 6).
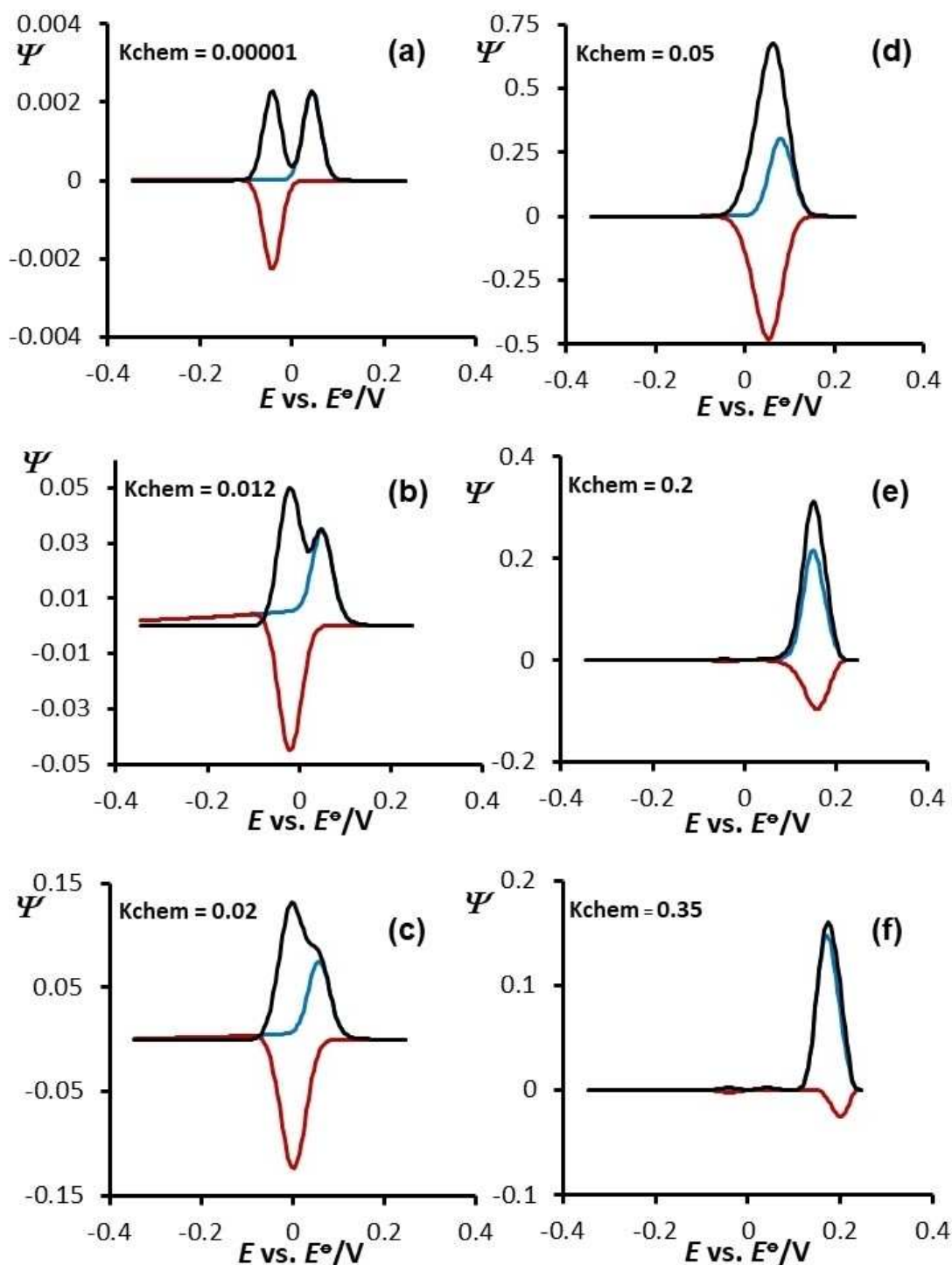
Fig. 6. *Surface ECE mechanism: Square-wave voltammetric patterns simulated for both electrode steps taking place at same potential:* Effect of the chemical kinetic parameter K_{chem} to the features of simulated SW voltammograms. The values of K_{chem} are given in the charts. In all simulations, the values of KI and KII were set to 10. Other simulation parameters were same as in Figure 1.

By increasing the rate of chemical reaction up to $K_{chem} = 0.05$, we observe simultaneous enlargement of all SWV current components, which is followed by vanishing of splitting phenomenon for $K_{chem} > 0.03$. Further increase of the rate of chemical reaction (for $K_{chem} > 0.075$) produces single-peak SW voltammograms, whose all

current components decrease, as typical for a surface ECirr mechanism [10]. An increase of K_{chem} from 0.03 to 0.5 affects also the position of net SW peak that shifts towards more positive potentials for $+59\ mV/\log(K_{chem})$ in this region of rates of irreversible chemical reaction. The only thing that distinguishes two-step surface ECE

mechanism from simple surface EC or CE mechanisms is the appearance of very small after-peaks appearing at more negative potentials than the major peak in such scenario. These small after-peaks are slightly visible in Figure 5c–d and Figure 6e–f, but they get more pronounced in the next elaborated surface EECrev mechanism.

4.3 C. Surface EEC$_{rev}$ Mechanism

4.3.1 V. Surface EEC$_{rev}$ Mechanism with Two Electrode Steps Separated for at Least 300 mV

In our very recent work [27] we presented detailed theoretical elaboration for the first time of a surface EEC$_{irr}$ mechanism under conditions of SWV. The surface EECrev mechanism ("rev" stands for "reversible") has not been elaborated so far under conditions of SWV. Therefore, we provide the readers entire MATHCAD file of this electrode mechanism in Supplementary Material of this work. SW voltammetric outputs of surface EEC$_{rev}$ mechanism are mainly affected by the two electrode kinetic parameters KI and KII. In addition, the equilibrium constant of follow-up chemical step $K_{eq} = k_f/k_b$, as well as the rate of follow-up chemical reaction expressed via K_{chem} ($K_{chem} = (k_f + k_b)/f$) also affect the features of calculated SW voltammograms. While the value of K_{eq} determines the equilibrium amount of redox active Red (ads) species, the rate of removal/resupply of Red(ads) species in the time frame of each potential pulse is governed by the value of chemical parameter K_{chem}. Indeed, the large number of parameters affecting the SW voltammograms at this redox mechanism can bring a very complex interplay. Here we focus only on several specific situations of this important two step surface mechanism.

As it has been shown in our recent work [29], for given values of KI, KII and K_{eq}, voltammetric patterns of "simple" surface ECrev systems are strongly affected by chemical rate constant K_{chem}. Since in EECrev mechanism, the chemical step is coupled to the final product of the two-step surface electrode reaction, we expect that any increase of K_{chem} will affect the voltammetric features of second electrode process (Peak II) only. Such an "ideal" scenario is presented in Figure 7, where an increase of K_{chem} is followed by a decrease of all SWV current components of Peak II only.

Remarkably, next to the Peak II that gets diminished in all current components by increasing of K_{chem}, a small "after-peak" emerges at more negative potentials (at about −0.5 V). This phenomenon was mentioned by the surface ECE mechanism featuring fast electron transfer, and it appears with higher intensity at surface EEC$_{rev}$ mechanisms featuring fast electron transfer at both electrode steps (Figure 8). Shown in Figure 8 is a series of SW voltammograms, calculated for both KI and KII = 4.50 (both electrode processes fall in region of fast electron transfer), for $K_{eq} = 100$, and for several values of chemical rate parameter K_{chem}. An initial increase of the
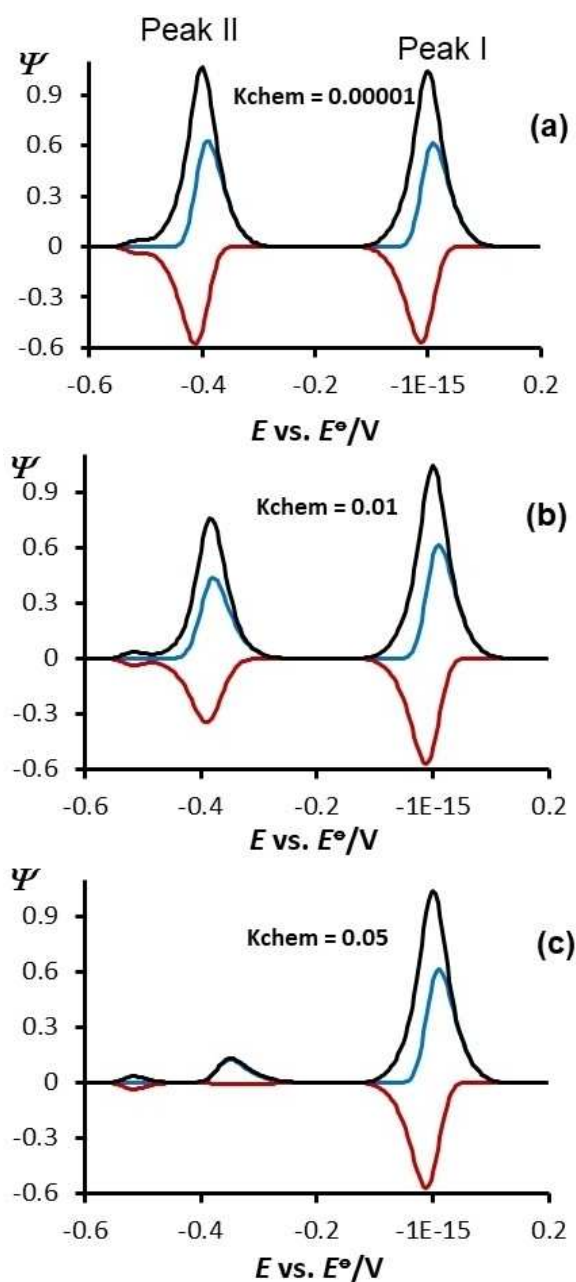

Fig. 7. **Surface EECrev mechanism**: Square-wave voltammetric patterns simulated at potential separation of −400 mV between the two electrode steps: Effect of the chemical kinetic parameter K_{chem} to the features of simulated SW voltammograms. The values of K_{chem} are given in the charts. In all simulations, the values of KI and KII were set to 0.316. Equilibrium constant $K_{eq} = 100$. Other simulation parameters were same as in Figure 1.

rate of follow-up chemical reaction (i.e. for K_{chem} values up to 0.01) produces significant enlargement of both current components of second electrode process. More pronounced increase is observed at reoxidation (backward) current components of calculated SW voltammograms (Figure 8a–d). In the same time, the position of backward (reoxidation) peak of second electrode step moves to more positive values (it shifts for 59 mV/log
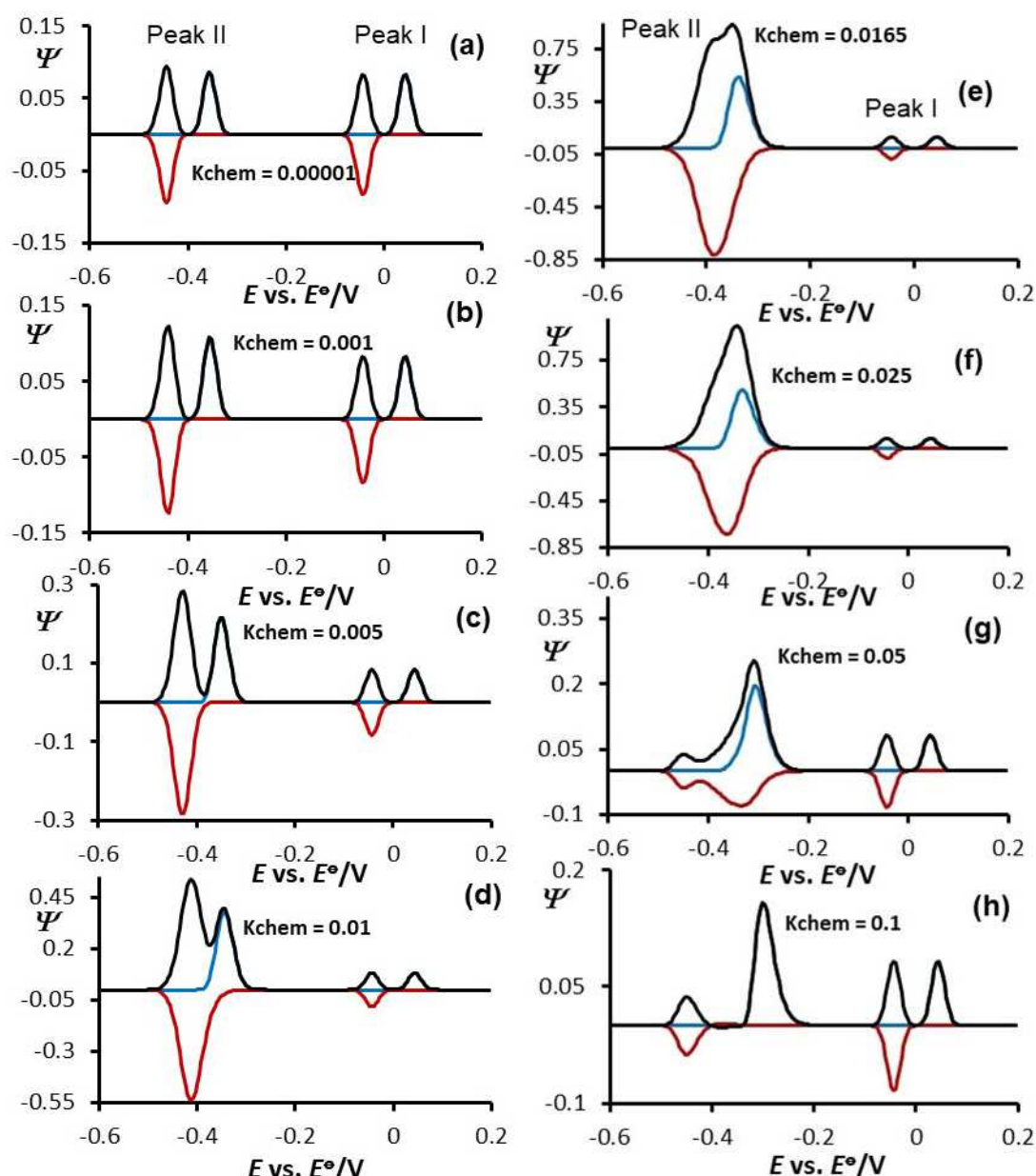
Fig. 8. **Surface EECrev mechanism**: Square-wave voltammetric patterns simulated at potential separation of −400 mV between the two electrode steps: Effect of the chemical kinetic parameter K_{chem} to the features of simulated SW voltammograms. The values of K_{chem} are given in the charts. In all simulations, the values of KI and KII were set to 4.47. Equilibrium constant $K_{eq} = 100$. Other simulation parameters were same as in Figure 1.

(K_{chem}) in the region of $0.005 < K_{chem} < 0.05$). The SWV splitting phenomenon at the second electrode process disappears for values of $K_{chem} > 0.02$. A further increase of K_{chem} produces patterns at second electrode step that are typical for a surface ECrev reaction (Figure 8f–h) [29]. Origin of the phenomena observed at second electrode step in Figure 8 is similar as that given for the surface ECE mechanism elaborated in this work. The only feature that distinguishes the SWV patterns of the two-step surface EECrev mechanism from "simple" one-step surface EC_{rev} systems [29] is seen in the existence of small after-peak that appears at surface EECrev mechanism for

values of $K_{chem} > 0.03$ (see Figure 8g–h). When considering the two-step surface EECrev mechanism, we should bear in mind that the supply/resupply of last electrode-active redox adsorbate (i.e. the Red(ads) species) comes from two sources: (a) electrochemically-from the first electrode step, but also (b) chemically-from the coupled chemical equilibrium. In addition, it is worth to mention that first electrode step of surface EECrev systems takes place (with much higher kinetics) at potentials defined for the second electrode step, too. Indeed, an interplay between kinetics of electron transfers of both electrode steps, and the high rates of coupled chemical reaction, can produce

These are not the final page numbers! ↗↗

some additional amount of Red(ads) prone to be re-oxidized at more negative potentials. This scenario, together with specific chronoamperometric features of surface reactions in SWV is probably the cause of existence of the "after-peak" observed at surface EEC$_{rev}$ mechanism (Figure 8g–h). It is worth to mention that such an event was not observed by the two-step surface EEC$_{irr}$ mechanism, as reported in [27].

4.3.2 VI: Surface EEC$_{rev}$ Mechanism with Both Electrode Steps Taking Place at Same Potential

When both electrode steps of a given surface EEC$_{rev}$ system happen at a same potential, then several scenarios are worth to be elaborated. Presented in Figures 9 and 10 are SW voltammograms, calculated for equilibrium constant of chemical step $K_{eq} = 10$. Shown at these voltammetric patterns is the effect of rate of follow-up chemical reaction in case of moderate (Figure 9) and fast (Figure 10) kinetics at both electrode steps of surface EEC$_{rev}$ mechanism. In first scenario (for $KI = KII = 1$), an increase of chemical rate parameter up to K_{chem} of 0.1 produces a minute decrease of all current components (Figure 9a–c).

For $K_{chem} > 0.1$, there is no longer effect of rate of follow-up chemical step and steady state SW voltammograms are observed, independent on K_{chem} (Figure 9c–d). The voltammetric patterns in Figure 9c–d imply that no efficient removal of Red(ads) happens in such scenario. Since the equilibrium constant K_{eq} regulates the equilibrium amount of Red(ads) species, SW voltammograms at Figure 9 suggest that even high rates of follow-up chemical step cannot convert significantly Red(ads) material to electroinactive product Z(ads). As both electrode steps happen at very same potential, continuous resupply of Red(ads) happens at all potential pulses via the coupled electrochemical steps. This is the most probable cause of SW voltammetric patterns observed at high equilibrium constant of follow-up chemical step (Figure 9c–d).

Shown in Figure 10 is the effect of rate of follow-up chemical reaction to calculated SW voltammograms of a surface EECrev mechanism featuring fast electrode transfer in both electrode steps ($KI = KII = 10$). In this scenario, up to K_{chem} values of about 0.01, the features of calculated SW patterns (Figure 10a–d) are similar to those explained in our recent work of one-step surface ECrev mechanism [29]. However, for $K_{chem} > 0.04$, steady state like SW voltammograms are obtained, whose features get independent on K_{chem} (Figure 10e–f). Interestingly, the current of backward (reoxidation) peak gets significantly higher values than that of forward (reduction) peak, for all values of K_{chem}. The ratio of absolute values of peak-current magnitudes of backward *vs.* forward peaks reaches a constant value of 0.8 for $K_{chem} > 0.03$ (Figure 10e–f). This is a unique pattern of a two-step surface EECrev mechanism, whose both electrode steps feature fast electrode kinetics. Therefore, this is a very specific
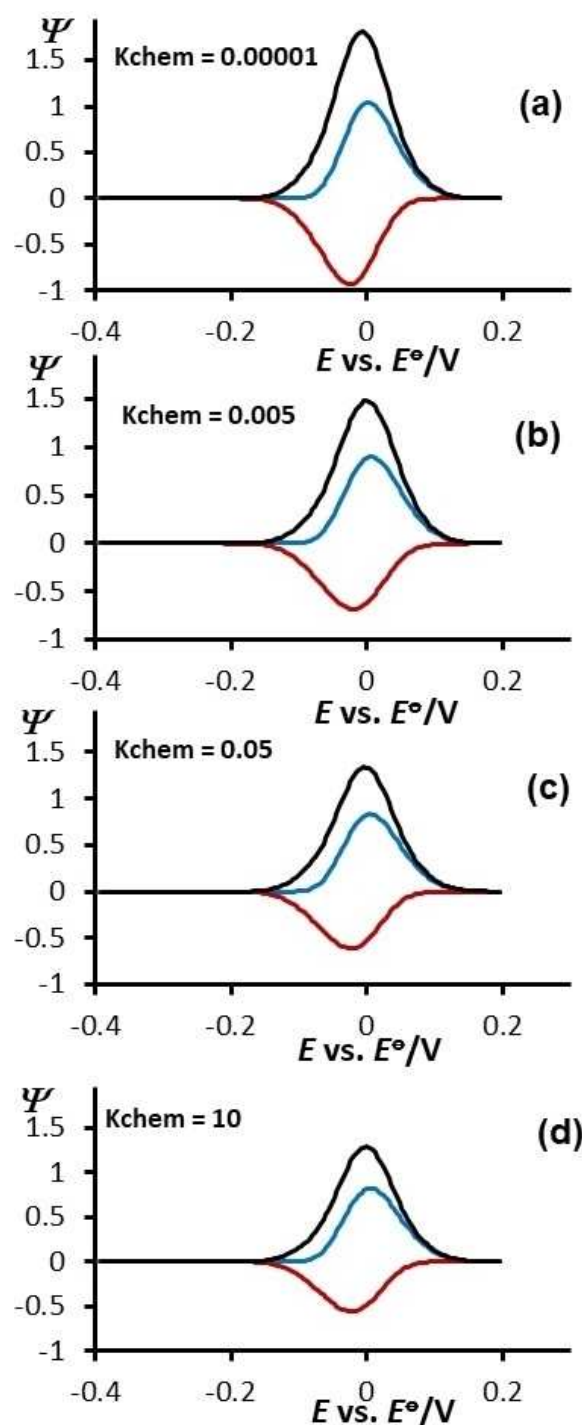

Fig. 9. **Surface EECrev mechanism**: Square-wave voltammetric patterns simulated for both electrode steps taking place at same potential: Effect of chemical kinetic parameter K_{chem} to the features of simulated SW voltammograms. The values of K_{chem} are given in the charts. In all simulations, the values of KI and KII were set to 1. Equilibrium constant K_{eq} was set to 10. Other simulation parameters were same as in Figure 1.

characteristic of this mechanism that distinguishes it from other two-step surface electrode mechanisms. The SW voltammetric patterns presented in Figure 10 can serve as
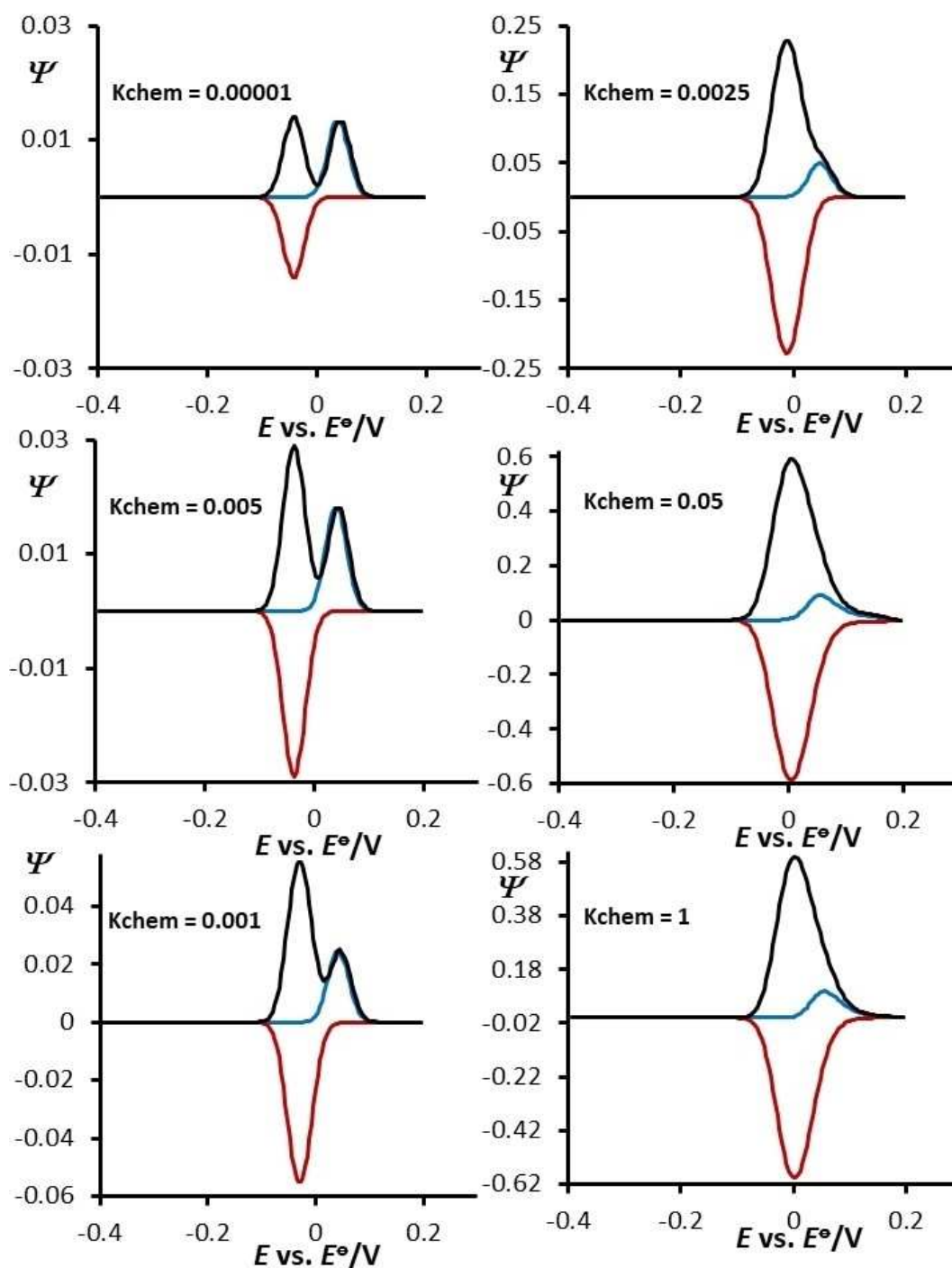
Fig. 10. Surface EECrev mechanism: Square-wave voltammetric patterns simulated for both electrode steps taking place at same potential: Effect of the chemical kinetic parameter K_{chem} to the features of simulated SW voltammograms. The values of K_{chem} are given in the charts. In all simulations, the values of KI and KII were set to 10. Equilibrium constant K_{eq} was set to 10. Other simulation parameters were same as in Figure 1.

a diagnostic criterion to recognize this particular mechanism, in case both electrode steps happen at same potential. Indeed, there are many more scenarios to be considered at this complex two-step mechanism. Especially complex for elaboration are the scenarios with small or moderate values of K_{eq} that will be completely

considered in our further work focused on this particular mechanism.

4.4 D. Surface Catalytic EEC' Mechanism

4.4.1 VII. Surface Catalytic EEC' Mechanism with two Electrode Steps Separated for at Least 300 mV

Many aspects of the two-step surface catalytic EEC' mechanism are elaborated in our work in [26]. In the current work, we focus on just some specific features of this mechanism in SWV in order to compare it and distinguish it from other similar surface mechanisms. The catalytic mechanism in voltammetry is a specific event that comprises regeneration of initial reactant of a defined electrode step. This happens via irreversible chemical reaction of final product of that electrode step with a given (electrochemically inactive) substrate "Y". Shown in Figure 11 is a series of calculated SW voltammograms representing the effect of catalytic parameter K_{chem} in scenario of moderate kinetics of electron transfer at both electrode steps ($KI = KII = 0.5$).

An increase of reduction (forward) and a concomitant decrease of oxidation (backward) current branches at SW voltammograms of second electrode step (Peak II), produced at increased rates of catalytic reaction, is recognizable feature of this particular mechanism. In addition, this phenomenon is associated by a simultaneous enlargement of net SWV peak currents, too (Figure 11b–d). For significant values of chemical catalytic parameter K_{chem}, both reduction and oxidation SWV current components get identical sign of currents measured. In the same time, both current branches get close to each other with their magnitudes (Figure 11d). This event happens when the rate of catalytic reaction is much higher than the rate of redox electrode transformation at the working electrode surface. Under such circumstances, a multiple reuse of starting electroactive material of second electrode step occurs during the time-frame of current measuring at given potential pulses. Consequently, the measured net SWV currents increase in proportion to K_{chem} [26,32]. It is worth mentioning that even at very high rates of regenerative catalytic reaction, we observe in SWV always a well-defined net SW peak (Figure 11b–d). This happens because of differential nature in defining the net current component in SWV [10,11,40]. Reported phenomenon is also linked to the magnitude of SW amplitude. In SWV, the forward and backward current components get always separated to some extent if SW amplitudes bigger than 10 mV are applied [32].

Voltammetric patterns showing the effect of rate of catalytic (regenerative) reaction in scenario of two "split net SWV peaks" is given in Figure 12. Noticeably, the features we observe at the second electrode step (up to K_{chem} values of 0.01) are not typical for surface EC' mechanisms [10,14,32]. Specifically, an increase of K_{chem} from 0.001 to 0.01 (Figure 12a–c) produces attributes to the current components of second electrode step (Peak II) that resemble to those of a surface EC mechanism [29,35]. A possible cause of observing such phenomenon is seen in the interplay between chemical rate parameter K_{chem} and the dimensionless kinetic parameters KI and
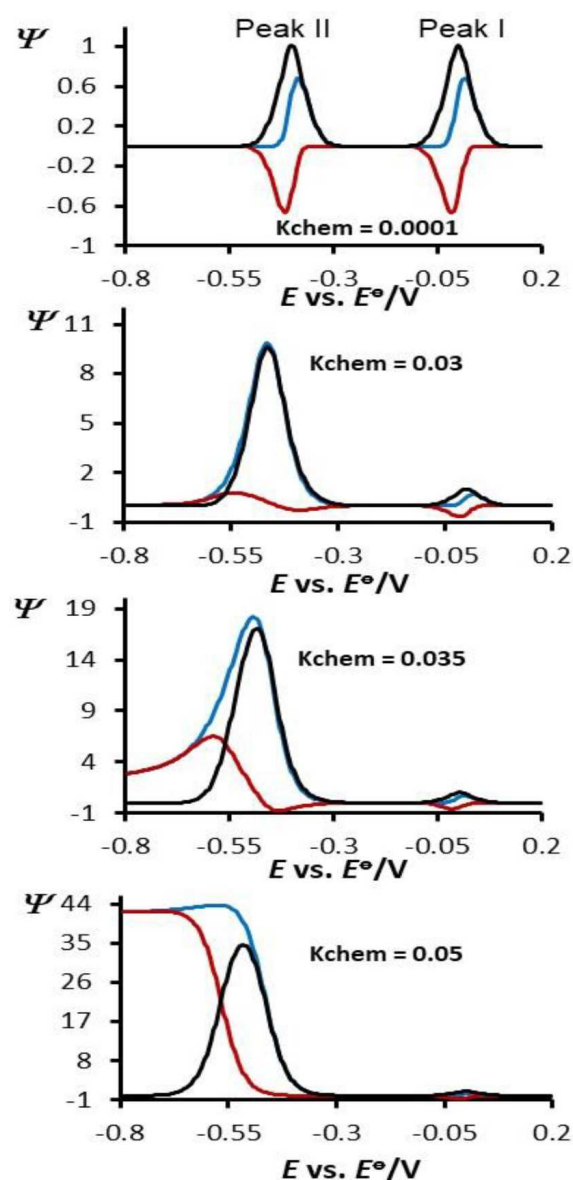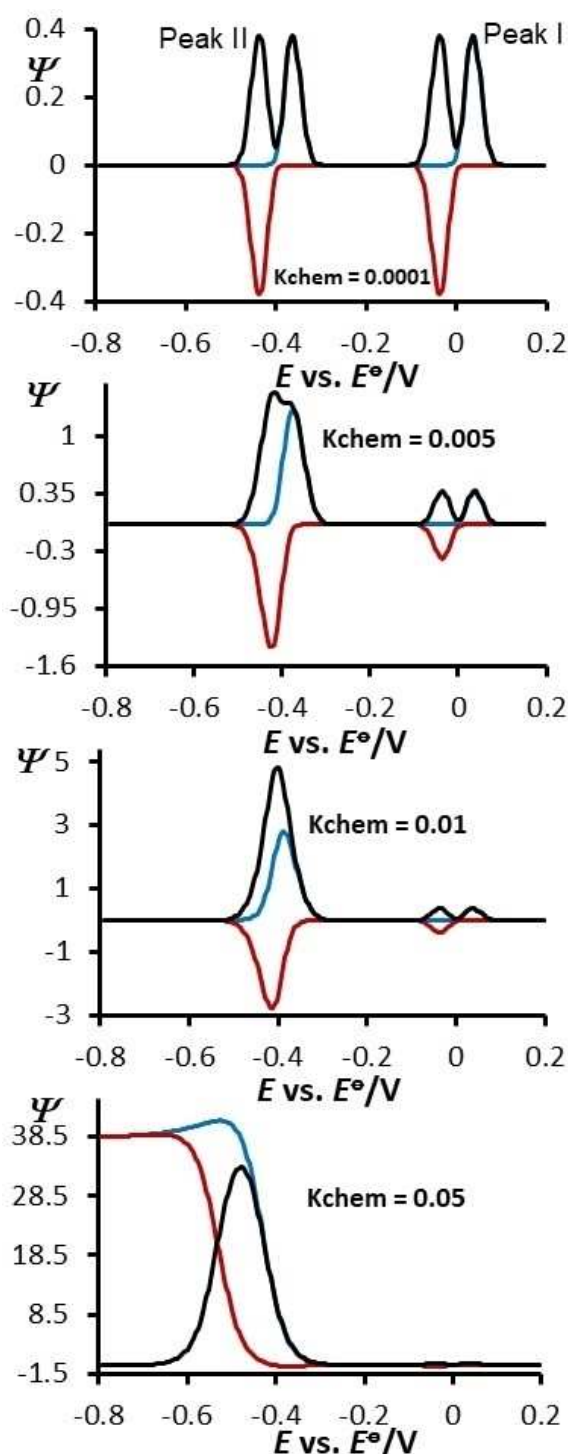

Fig. 11. Surface catalytic EEC' mechanism: Square-wave voltammetric patterns simulated at potential separation of −400 mV between the two electrode steps: Effect of the chemical kinetic parameter K_{chem} to the features of simulated SW voltammograms. The values of K_{chem} are given in the charts. In all simulations, the values of KI and KII were set to 0.5. Other simulation parameters were same as in Figure 1.

KII. Redox reactant of second electrode step in mechanism (4) (i.e. Int(ads)), is obtained in two ways: (a) electrochemically (via electrode transformation in first electrode step), but also (b) chemically via regenerative reaction of Red(ads) and the substrate "Y". It means, there are three different processes in which Int(ads) is involved in the same time. Indeed, such an event can produce a complex interplay between both electrode parameters KI and KII and the chemical catalytic parameter K_{chem}. This interplay between the three kinetic parameters can contribute to the uncommon voltammet-

Fig. 12. **Surface catalytic EEC' mechanism**: Square-wave voltammetric patterns simulated at potential separation of −400 mV between the two electrode steps: Effect of the chemical kinetic parameter K_{chem} to the features of simulated SW voltammograms. The values of K_{chem} are given in the charts. In all simulations, the values of KI and KII were set to 2. Other simulation parameters were same as in Figure 1.

ric patterns observed in Figure 12a–c. Only at significant rates of regenerative reaction (i.e. for values of $K_{chem} >$

0.02) we observe features at second SWV peak (Peak II) typical of surface catalytic EC' mechanism (Figure 12d). When both electrode processes of first and second electrode step are separated for at least 300 mV, we can explore the very same set of analysis elaborated in [14,26,32] in order to get access to kinetic and thermodynamic parameters relevant to second electrode step of a surface catalytic EEC' mechanism.

4.4.2 VIII. Surface Catalytic EEC' Mechanism with Both Electrode Steps Taking Place at Same Potential

A rather complex interplay between KI, KII and K_{chem} is observed when both electrode steps of a surface catalytic EEC' mechanism occur at a same potential (Figure 13 and Figure 14). The voltammetric patterns presented in Figure 13 are calculated for KI = KII = 0.5 (region of moderate electron transfer at both electrode reactions), while SW voltammograms at Figure 14 are calculated for KI = KII = 4 (i.e. fast electron transfer rate at both electrode steps).

Since the chemical catalytic parameter K_{chem} under such circumstance influences not only the second, but also the first electrode step, it produces a very complex SW voltammetric pattern. The effect of chemical catalytic parameter K_{chem} to the features of SW voltammograms calculated for KI = KII = 0.5 resembles much more to its effect at surface EC mechanism [29,35] rather than at surface catalytic EC' [14,32] mechanism (Figure 13a–d). Interestingly, for K_{chem} of about 0.05 we see that the net SW response features two peaks (Figure 13e), while the SW voltammograms start getting shape typical of surface catalytic mechanism [32] by further increase of K_{chem} (Figure 13f). The phenomena met in Figure 13 can serve as diagnostic criteria to distinguish the two-step surface catalytic EEC' mechanism from the one-step surface catalytic EC' systems [32].

The SW voltammetric patterns representing the effect of rate of catalytic reaction when both electrode processes of surface catalytic EEC' mechanism feature fast electron transfer (KI = KII = 4) also differ from the corresponding features met by the simple one-step surface EC' mechanism [32]. As shown in Figure 14a–d, an increase of K_{chem} from 0.001 to 0.065 produces a simultaneous increase of all SWV current components, with more pronounced enlargement by the backward (reoxidation) SW current branch. For instance, the ratio of the magnitude of peak currents of backward vs forward peak changes from 1.0 (for K_{chem} of 0.001) to 1.85 (for K_{chem} of 0.025). In this range of rates of the regenerative reaction, the features of calculated SW voltammograms resemble to those of a surface ECrev reaction [29]. Even at K_{chem} values larger than 0.08 (Figure 14e–f), we observe voltammetric patterns as typical of a surface catalytic mechanism [32]. The voltammetric patterns presented in Figure 14 can be seen as additional valuable criterion to distinguish the two-step surface catalytic EEC' mechanism from the one-step
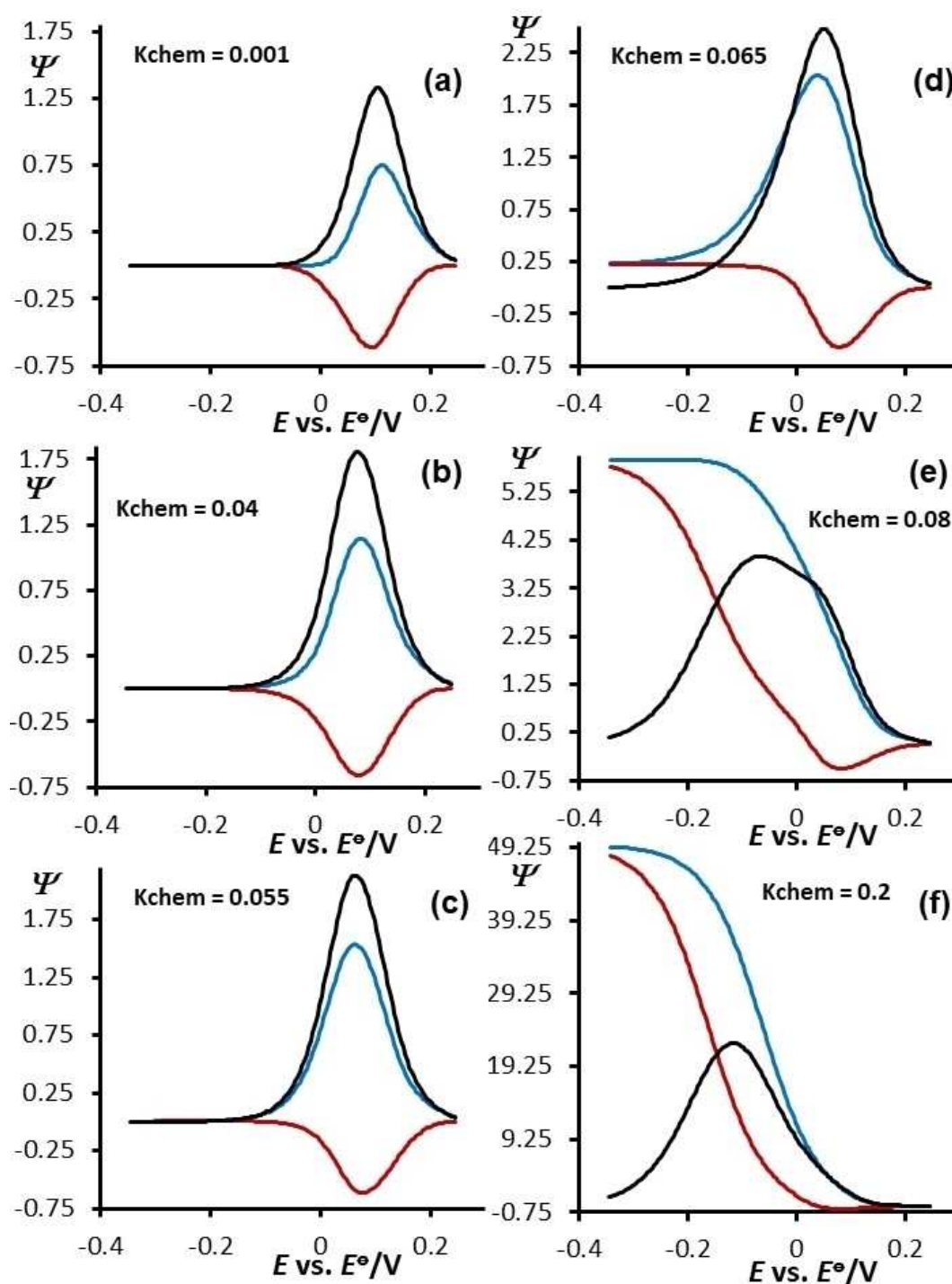
Fig. 13. **Surface catalytic EEC' mechanism**: Square-wave voltammetric patterns simulated for both electrode steps taking place at same potential: Effect of chemical kinetic parameter K_{chem} to the features of simulated SW voltammograms. The values of K_{chem} are given in the charts. In all simulations, the values of KI and KII were set to 0.5. Other simulation parameters were same as in Figure 1.

simple EC' mechanism, but also from all other two-step surface electrode mechanisms elaborated in this work.

5 Conclusions

As we have seen from the large number of calculated SW voltammograms presented in this work, the considered two-step surface mechanisms coupled to chemical reactions can produce very complex voltammetric patterns. The situation gets even more complicated when both
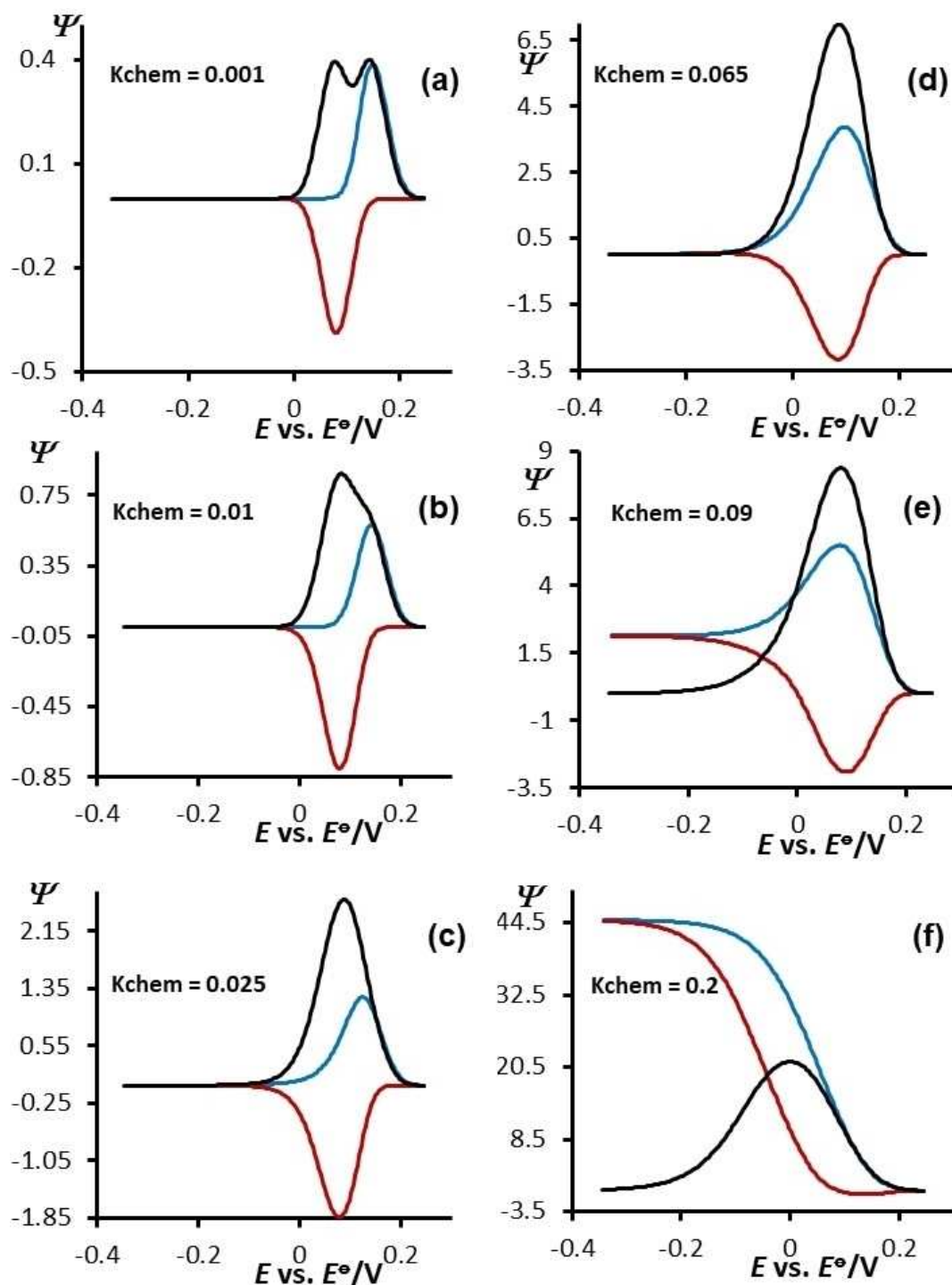
Fig. 14. **Surface catalytic EEC' mechanism**: Square-wave voltammetric patterns simulated for both electrode steps taking place at same potential: Effect of the chemical kinetic parameter K_{chem} to the features of simulated SW voltammograms. The values of K_{chem} are given in the charts. In all simulations, the values of KI and KII were set to 4. Other simulation parameters were same as in Figure 1.

electrode steps, with one or both of them coupled by additional chemical reaction, occur at a same potential. Indeed, a primary goal in experimental scenario of all these mechanisms is to understand whether the electrode step is composed of two successive steps, or it is a two-electron transformation happening in one step. As it is

shown in Figures 3 to 14, the features of all simulated voltammograms relevant to two-step surface ECE, EE-Crev or EEC' mechanisms strongly depend on the value of chemical parameter K_{chem}. In mechanisms (2), (3) and (4), the chemical parameter K_{chem} is time (frequency) dependent parameter. However, for all two-step mecha-

nisms (2–4) coupled with chemical reaction, the value of K_{chem} is also a function of concentration of "Y"-c(Y). As we mentioned, the SW frequency affects simultaneously not only kinetics of chemical reactions, but also the kinetics of electrochemical reactions of studied redox adsorbates, too. Consequently, the frequency (or time) analysis in voltammetric experiments of electrode reactions coupled to chemical reactions, produces a rather complex interplay to all kinetic parameters. Therefore, a better scenario of reproducing the voltammetric patterns in Figures 3 to 14 is to make an analysis by modifying the concentration of "Y", under conditions of constant frequency and constant SW amplitude. From the experimental voltammetric outputs obtained by altering the concentration of "Y" only, we can recognize the type of a given particular two-step surface mechanism. This is achievable, since all of the mechanisms (2), (3) and (4) have quite specific SW voltammetric patterns, regardless whether both steps occur at quite different or at very same potential. When both electrode steps of a given two-step surface mechanism are separated for 300 mV or even more, then we can explore the methods elaborated in [8, 10, 14, 28, 29, 31, 32, 36] to get insight to all relevant kinetic and thermodynamic parameters. The method of "quasireversible maximum" [10] can be explored to get insight into kinetics of electrode reactions in case of two well-separated SW peaks at all elaborated two-step mechanisms, except at the surface EECrev mechanism featuring high values of equilibrium constant of follow up chemical step [29]. In [29] we have shown that the rate of follow-up chemical step affects the position of "quasireversible maximum" phenomenon, for values of equilibrium constant of follow-up step larger than 10. For the surface EECrev mechanism, we advise the readers to use the methodology proposed in [29] for the determination of kinetics of electrode reactions, but also the kinetics and thermodynamics of chemical step, too. By the surface ECE mechanism and the surface EEC' mechanism, the electrode kinetics (accessed via "quasireversible maximum" feature) of both steps is not affected by the chemical rate parameters. However, when both electrode steps occur at the same potential, then we can get limited access to the parameters relevant to electrode steps or chemical reactions, due to the complex mutual interplay of all kinetic parameters. Indeed, one needs more complex algorithm to evaluate relevant kinetics and thermodynamics parameters in such scenario. Anyway, the principles elaborated in this work can explain many experimental features met in the voltammetry of many enzymes and other surface-active redox compounds [3–5, 10, 60–64]. For the simple "two-step" mechanism in square-wave voltammetry, one can also get more impressions from the recent papers of Lovric and Komorsky Lovric reported in [65, 66].

References
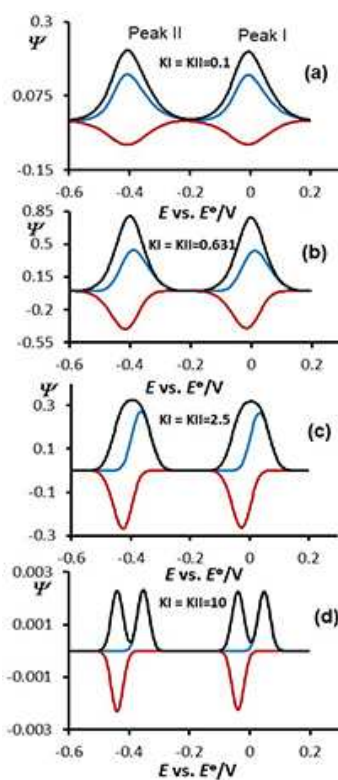
[1] P. N. Barlett, *Bioelectrochemistry: Fundamentals, experimental techniques and application*, Wiley, Chichester, **2008**.

[2] C. Leger, P. Bertrand, *Chem. Rev.* **2008**, *108*, 2379.

[3] F. A. Arsmstrong, *Electrifying metalloenzymes* in: *Metalloproteins: Theory, calculations and experiments* (A. E. Cho, W. A. Goddar III, eds), CRC Press, Taylor&Francis Group, London, New York, **2015**.

[4] F. A. Armstrong, Applications of voltammetric methods for probing the chemistry of redox proteins In: *Bioelectrochemistry: Principles and practice* (G. Lenaz, G. Milazz eds), Birkhauser Verlag AG, Basel, **1997**.

[5] F. A. Armstrong, *Voltammetry of proteins.* in: *Encyclopedia of electrochemistry* (A. J. Bard, M. Stratmann, G. S. Wilson, eds), Wiley VCH, Weinheim, **2002**.

[6] F. A. Armstrong, H. A. Heering, J. Hirst, *Chem. Soc. Rev.* **1997**, *26*, 169.

[7] C. Leger, S. J. Elliott, K. R. Hoke, L. J. C. Jeuken, A. K. Jones, F. A. Arsmtrong, *Biochem.* **2003**, *42*, 8653.

[8] R. Gulaboski, V. Mirceski, I. Bogeski, M. Hoth, *J. Solid State Electrochem.* **2012**, *16*, 2315.

[9] R. Gulaboski, P. Kokoskarova, S. Mitrev, *Electrochim. Acta* **2012**, *69*, 86.

[10] V. Mirceski, S. Komorsky-Lovric, M. Lovric, *Square-wave voltammetry, Theory and application*, Springer, Berlin, Germany, **2007**.

[11] M. Lovric, "Square-wave voltammetry," in *Electroanalytical Methods*, F. Scholz, Ed. Springer, Berlin, Germany, 2nd edition, **2010**.

[12] V. Mirceski, R. Gulaboski, *Croat. Chem. Acta* **2003**, *76*, 37.

[13] V. Mirceski, R. Gulaboski, *Maced. J. Chem. Chem. Eng.* **2014**, *33*, 1.

[14] V. Mirceski, R. Gulaboski, M. Lovric, I. Bogeski, R. Kappl, M. Hoth, *Electroanalysis* **2013**, *25*, 2411.

[15] R. Gulaboski, M. Lovric, V. Mirceski, I. Bogeski, M. Hoth, *Biophys. Chem.* **2008**, *137*, 49.

[16] R. Gulaboski, M. Lovric, V. Mirceski, I. Bogeski, M. Hoth, *Biophys. Chem.* **2008**, *138*, 130.

[17] A. Molina, J. Gonzales, Pulse voltammetry in *physical electrochemistry and electroanalysis, in Monographs in electrochemistry* (F. Scholz, ed.), Berlin Heidelber, Springer, **2016**.

[18] R. G. Compton, C. E. Banks, *Understanding voltammetry, 2nd Edition*, Imperial College Press, London, UK, **2011**.

[19] A. J. Bard, L. R. Faulkner, *Electrochemical methods. Fundamentals and applications, 3rd edition*, John Wiley & Sons, Inc. **2004**.

[20] H. Sies, L. Parker, *Quinones and quinone enzymes*, in *Methods in enzymology*, Academic Press, UK, **2004**.

[21] R. Hille, *Trends Biochem. Sci.* **2002**, *27*, 360.

[22] U. Ermler, W. Grabarse, S. Shima, M. Goubeaud, R. K. Thauer, *Curr. Opin. Struct. Biol.* **1998**, *8*, 749.

[23] M. Kobayashi, S. Shimizu, *Eur. J. Biochem.* **1999**, *261*, 1.

[24] D. C. Crans, J. J. Smee, E. Galdamauskas, L. Yang, *Chem. Rev.* **2004**, *104*, 849.

[25] R. Gulaboski, *J. Solid State Electrochem.* **2009**, *13*, 1015.

[26] R. Gulaboski, L. Mihajlov, *Biophys. Chem.* **2011**, *155*, 1.

[27] P. Kokoskarova, V. Maksimova, M. Janeva, R. Gulaboski *Electroanalysis*, **2019**, doi.org/10.1002/elan.201900225.

[28] R. Gulaboski, P. Kokoskarova, S. Petkovska, *Croat. Chem. Acta* **2018**, *91*, 377.

[29] R. Gulaboski, M. Janeva, V. Maksimova, *Electroanalysis* **2019**, doi.org/10.1002/elan.201900028.

[30] V. Mirceski, R. Gulaboski, I. Kuzmanovski, *Bull. Chem. Technol. Macedonia* **1999**, *18*, 57.

[31] R. Gulaboski, V. Mirceski, M. Lovric, I. Bogeski, *Electrochem. Commun.* **2005**, *7*, 515.

[32] R. Gulaboski, V. Mirceski, *Electrochim. Acta* **2015**, *167*, 219.

[33] V. Mirceski, D. Guzijewski, K. Lisichkov, *Electrochim. Acta* **2013**, *114*, 667.

[34] D. Guziejewski, V. Mirceski, D. Jadresko, *Electroanalysis* **2015**, *27*, 67.

[35] R. Gulaboski, *Electroanalysis* **2019**, *31*, 545.

[36] R. Gulaboski, M. Janeva, V. Maksimova, *Electroanalysis* **2019**, *31*, https://doi.org/10.1002/elan.201900028.

[37] V. Mirceski, M. Lovric, *Electroanalysis* **1997**, *9*, 1283.

[38] M. Lovric, *J. Electroanal. Chem.* **1983**, *153*, 1.

[39] R. Meunier-Prest, E. Laviron, *J. Electroanal. Chem.* **1996**, *410*, 133.

[40] J. G. Osteryoung, J. J. O'Dea, *Square-Wave Voltammetry, Electroanalytical chemistry: a series of advances.* Marcel Dekker, Inc: New York, **1986**.

[41] A. B. Miler, R. G. Compton, *J. Phys. Chem. B* **2000**, *104*, 5331.

[42] J. J. O'Dea, J. G. Osteryoung, *Anal. Chem.* **1997**, *69*, 650.

[43] A. Molina, C. Serna, M. López-Tenés, M. M. Moreno, *J. Electroanal. Chem.* **2005**, *576*, 9.

[44] J. Galvez, R. Saura, A. Molina, T. Fuente, *J. Electroanal. Chem.* **1982**, *139*, 15.

[45] J. Osteryoung, J. J. O'Dea, *Square-wave voltammetry, in Electroanalytical Chemistry*, A. J. Bard, Ed. Marcel Dekker, New York, NY, USA, **1986**, *14*, 209.

[46] E. Laborda, J. Gonzales, A. Molina, *Electrochim. Acta* **2014**, *43*, 25.

[47] J. J. O'Dea, J. G. Osteryoung, *Anal. Chem.* **1993**, *65*, 3090.

[48] J. J. O'Dea, J. Osteryoung, R. A. Osteryoung, *Anal. Chem.* **1981**, *53*, 695.

[49] M. Lovric, D. Jadresko, *Electrochim. Acta* **2010**, *55*, 948.

[50] F. Ammar, J. M. Saveant, *J. Electroanal. Chem.* **1973**, *47*, 215.

[51] J. Galvez, M. L. Alcaraz, S. M. Park, *J. Electroanal. Chem.* **1989**, *266*, 1.

[52] M. Lovric, S. Komorsky-Lovric, *Intern. J. Electrochem.* **2012**, https://doi.org/10.1155/2012/596268.

[53] S. Komorsky-Lovric, M. Lovric, *J. Electroanal. Chem.* **2011**, *660*, 22.

[54] P. Song, A. C. Fisher, J. D. Wadhawan, J. J. Cooper, H. J. Ward, N. S. Lawrence, *RSC Adv.* **2016**, *6*, 70237.

[55] V. Mirceski, E. Laborda, D. Guziejewski, R. Compton, *Anal. Chem.* **2013**, *85*, 5586.

[56] V. Mirceski, D. Guzijewski, M. Bozem, I. Bogeski, *Electrochim. Acta* **2016**, *213*, 520.

[57] C. Batchelor-McAuley, E. Katelhon, E. O. Barnes, R. G. Compton, E. Laborda, A. Molina, *ChemistryOpen* **2015**, *4*, 224.

[58] C. Bonazzola, G. Gordillo, *Electrochim. Acta* **2016**, *213*, 613.

[59] P. Dauphin-Durcharme, N. Arroyo-Curras, M. Kurnik, G. Ortega, H. Li, K. W. Plaxco, *Langmuir* **2017**, *33*, 4407.

[60] F. A. Armstrong, H. A. Heering, J. Hirst, *Chem. Soc. Rev.* **1997**, *26*, 169.

[61] F. A. Armstrong, R. M. Evans, S. V. Hexter, B. J. Murphy, M. M. Roessler, Ph. Wulff, *Acc. Chem. Res.* **2016**, *49*, 884.

[62] P Bertrand, B. Frangioni, S. Dementin,, M. Sabaty, P. Arnoux, B. Guigliarelli, D. Pignol, Ch. Léger, *J. Phys. Chem. B* **2007**, *111*, 10300.

[63] H. J. Wijma, L. J. C. Jeuken, M. Ph. Verbeet, F. A. Armstrong, G. W. Canters, *J. Am. Chem. Soc.* **2007**, *129*, 8557.

[64] L. J. C. Jeuken, S. D. Connell, P. J. F. Henderson, R. B. Gennis, S. D. Evans, R. J. Bushby, *J. Am. Chem. Soc.* **2006**, *128*, 1711.

[65] S. Komorsky Lovric, M. Lovric, *Int. J. Electrochem. Sci.* **2014**, *9*, 435.

[66] M. Lovric, S. Komorsky-Lovric, *Croat. Chem. Acta* **2012**, *85*, 569.

FULL PAPER

M. Janeva, P. Kokoskarova, V. Maksimova, R. Gulaboski*

1 – 20

Square-wave Voltammetry of Two-step Surface Electrode Mechanisms Coupled with Chemical Reactions – a Theoretical Overview